Bioorganic & Medicinal Chemistry Letters 20 (2010) 6030–6033

Contents lists available at ScienceDirect

Bioorganic & Medicinal Chemistry Letters

journal homepage: www.elsevier.com/locate/bmcl

Discovery of pyrrolopyridazines as novel DGAT1 inhibitors

Brian M. Fox [a], Kiyosei Iio [b], Kexue Li [a], Rebeka Choi [a], Takashi Inaba [b], Simon Jackson [a], Shoichi Sagawa [b], Bei Shan [a], Masahiro Tanaka [b], Atsuhito Yoshida [b], Frank Kayser [a,*]

[a] Amgen Inc., Amgen South San Francisco, 1120 Veterans Boulevard, South San Francisco, CA 94080, USA
[b] Japan Tobacco Inc., Central Pharmaceutical Research Institute, 1-1, Murasaki-cho Takatsuki, Osaka 569 1125, Japan

ARTICLE INFO

Article history:
Received 13 July 2010
Revised 12 August 2010
Accepted 12 August 2010
Available online 18 August 2010

Keywords:
DGAT1 inhibitors
Pyrrolopyridazines
DGAT1
Acyl CoA:diacylglycerol acyltransferase

ABSTRACT

A new structural class of DGAT1 inhibitors was discovered and the structure–activity relationship was explored. The pyrrolotriazine core of the original lead molecule was changed to a pyrrolopyridazine core providing an increase in potency. Further exploration resulted in optimization of the propyl group at C7 and the discovery that the ester at C6 could be replaced by five-membered heterocyclic rings. The analogs prepared have DGAT1 IC_{50} values ranging from >10 μM to 48 nM.

Acyl CoA:diacylglycerol acyltransferase (DGAT) is a microsomal enzyme widely expressed in mammalian tissues that catalyzes the esterification of 1,2-diacylglycerol with fatty acyl CoA to form triglycerides at the endoplasmic reticulum.[1,2] Two DGAT enzymes, DGAT1 and DGAT2, have been identified.[3–5] Both DGAT1 and DGAT2 catalyze the formation of triglyceride from diacylglycerol and fatty acyl CoA but they share no homology. In fact, DGAT1 is part of the acyl CoA:cholesterol acyltransferase (ACAT) gene family consisting of enzymes that synthesize cholesterol esters from cholesterol and fatty acyl CoA substrates. Mouse DGAT1 shares 20% identity with mouse ACAT1.[3] Dgat1 null mice (Dgat1−/−) are lean and resistant to diet-induced obesity.[6] Total triglyceride and leptin levels are lower in Dgat1−/− mice compared to their wild type littermates and they have lower glucose and insulin levels after a glucose tolerance test, indicating that Dgat1−/− mice have increased insulin sensitivity. The totality of data indicates that loss of DGAT1 activity can counteract obesity and obesity-induced diabetes.[1,6,7]

Disorders or imbalances in triglyceride metabolism are implicated in the pathogenesis of a variety of diseases and risk factors including obesity, insulin resistance syndrome, type II diabetes, dyslipidemia, metabolic syndrome and coronary heart disease.[7–14] The finding that multiple enzymes catalyze the synthesis of triglyceride from diacylglycerol provides the opportunity to modulate one catalytic mechanism of this biochemical reaction to achieve therapeutic results in an individual with minimal adverse side effects. Compounds that inhibit the conversion of diacylglycerol to triglyceride by specifically inhibiting the activity of the human homolog of DGAT1 may find use in lowering corporeal concentrations and absorption of triglycerides, thereby therapeutically counteracting the pathogenic effects caused by abnormal metabolism of triglycerides in these disorders.

A high-throughput screen (HTS) of our small molecule library resulted in the identification of pyrrolotriazine **1** as a novel, moderately potent DGAT1 inhibitor (Fig. 1). Early work exploring cores similar to pyrrolotriazine **1** resulted in the discovery of pyrrolopyridazine **2a** possessing increased DGAT1 potency, as well as improved selectivity against ACAT1. We wished to improve the selectivity over ACAT1 in order to study the effect of DGAT1 inhibition without the need to deconvolute the contribution from each enzyme in any potential in vivo results. This report will focus on the synthesis of pyrrolopyridazine derivatives **2a** and the evaluation of their potency in DGAT1 biochemical[15] and cellular assays[16] and their selectivity in an ACAT1 biochemical assay.[17]

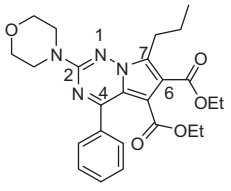

1
DGAT1 IC_{50} = 0.25 μM
ACAT1 IC_{50} = 0.5 μM

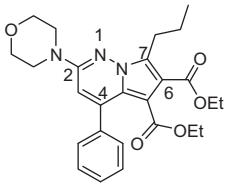

2a
DGAT1 IC_{50} = 0.12 μM
ACAT1 IC_{50} = 1.3 μM

Figure 1. Structures of original screening hit pyrrolotriazine **1** and pyrrolopyridazine **2a**.

* Corresponding author.
E-mail address: fkayser@amgen.com (F. Kayser).

0960-894X/$ - see front matter © 2010 Elsevier Ltd. All rights reserved.
doi:10.1016/j.bmcl.2010.08.066

Preparation of analogs **2a–w** (Table 1) and **9a–e** (Table 2) possessing a phenyl group at C4 began by treatment of phenylmaleic anhydride (**5**) with hydrazine followed by reaction with $POCl_3$ to provide dichloropyridazine **6** (Scheme 1). Displacement of the chloride in the 6-position with secondary amines followed by hydrogenation provided 5-phenylpyridazines **8**. Selective N-alkylation with various halides followed by 1,3-dipolar addition of the resulting ylide to diethyl acetylenedicarboxylate[18] provided pyrrolopyridazine analogs **2a–w** and **9a–e**. The synthesis of analogs **9f–h** containing substituted phenyls at C4 of the pyrrolopyridazine core required the preparation of arylmaleic anhydrides **5** that was accomplished by the condensation of benzonitriles **3** with glyoxylic acid followed by the hydrolysis of the resulting nitriles **4** (Scheme 1). Conversion of anhydrides **5** into pyrrolopyridazines **9f–h** was accomplished as described for analogs **2a–w** and **9a–e**.

Table 1
DGAT1 and ACAT1 IC_{50} values of **2a–w**

Compd	R	DGAT1 IC_{50} (μM)	ACAT1 IC_{50} (μM)
2a	Propyl	0.12 ± 0.06[a]	1.3 ± 0.04[b]
2b	Hydrogen	>3	
2c	Methyl	0.52	2.59
2d	Ethyl	0.24	2.17
2e	Allyl	0.075	1.4
2f	3,3,3-Trifluoropropyl	0.11	0.92
2g	Butyl	0.16	<0.3
2h	Pentyl	0.22	0.3
2i	Cyclopropyl	0.62	3.25
2j	Cyclobutyl	2.5	
2k[c]	3-Hydroxypropyl	>1.0	
2l	Methoxymethyl	0.24	8.75
2m	3-Methoxypropyl	0.27	2.56
2n[c]	3(*N*,*N*-Dimethylamino)propyl	>1	
2o	Phenyl	0.081	0.55
2p	3-OMe-phenyl	0.47	0.47
2q	3-Cl-phenyl	0.29	0.31
2r	4-Cl-phenyl	0.068	0.22
2s[d]	4-OH-phenyl	0.57	1.29
2t	4-OMe-phenyl	0.052	0.6
2u[e]	4-NH_2-phenyl	0.63	1.05
2v	4-Ph-phenyl	0.25	<0.3
2w	4-OBn-phenyl	0.060	<0.1

[a] $n = 17$.
[b] $n = 2$.
[c] Hydroboration oxidation of **2e** provided **2k** followed by mesylation and displacement with dimethylamine providing **2n**.
[d] Hydrogenolysis of **2w** provided **2s**.
[e] Hydrogenation of the corresponding nitroaryl provided **2u**.

Table 2
DGAT1 and ACAT1 IC_{50} values of **9a–m**

Compd	R_1	R_2	DGAT1 IC_{50} (μM)	ACAT1 IC_{50} (μM)
2a	Morpholin-4-yl	Phenyl	0.12 ± 0.06	1.3 ± 0.04
9a	*cis*-2,6-Dimethyl-morpholin-4-yl	Phenyl	>3	
9b	Azetidin-1-yl	Phenyl	1.36	1.49
9c	Pyrrolidin-1-yl	Phenyl	0.12	1.3
9d	Piperidin-1-yl	Phenyl	6.1	
9e	Dimethylamino	Phenyl	0.83	0.66
9f	Morpholin-4-yl	2-F-phenyl	0.57	1.49
9g	Morpholin-4-yl	3-F-phenyl	0.27	0.38
9h	Morpholin-4-yl	4-F-phenyl	0.29	0.99
9i	Morpholin-4-yl	Propyl	>3	
9j	Morpholin-4-yl	*t*-Butyl	>3	
9k	Morpholin-4-yl	Cyclobutyl	>3	
9l	Morpholin-4-yl	Cyclopentyl	>3	
9m	Morpholin-4-yl	Cyclohexyl	>3	

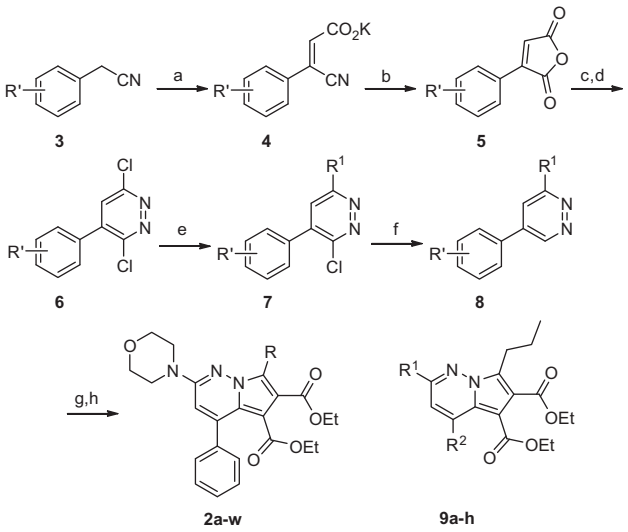

Scheme 1. Reagents and conditions: (a) glyoxylic acid, K_2CO_3, MeOH; (b) HCO_2H, H_2SO_4, reflux; (c) $NH_2NH_2{\cdot}HCl$, EtOH, H_2O, reflux; (d) $POCl_3$, reflux; (e) R^1H, *i*-Pr_2NEt, dioxane, reflux; (f) HCO_2NH_4, Pd/C, MeOH, 48 °C; (g) RCH_2X, CH_3CN, reflux; (h) diethyl acetylenedicarboxylate, TBAF, THF, EtOH, reflux.

Preparation of analogs **9i–m** containing alkyl groups at C4 of the pyrrolopyridazine core began by alkylating 3,6-dichloropyridazine (**10**) to provide 4-alkyl-3,6-dichloropyridazines **11** (Scheme 2).[19] Conversion of pyridazines **11** to the corresponding 4-alkylpyrrolopyridazines **9i–m** was accomplished using the chemistry shown in Scheme 1.

Selective hydrolysis of **2a** using NaOH in EtOH and H_2O provided the carboxylate. Subsequent conversion to the acid chloride, displacement with hydroxyamidines and cyclization in the presence of TBAF provided 1,2,4-oxadiazoles **12a–n** (Scheme 3).

Systematic exploration of the pyrrolopyridazine SAR included replacing the 7-propyl group of **2a** with various alkyl and aryl groups to provide analogs **2b–w** (Table 1). Propyl was found to be the optimal chain length for DGAT1 potency although larger and more lipophilic groups such as trifluoropropyl **2f**, butyl **2g** and pentyl **2h** had similar IC_{50} values. Sterically more demanding

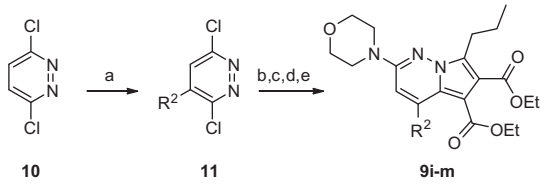

Scheme 2. Reagents and conditions: (a) R^2CO_2H, H_2SO_4, $AgNO_3$, H_2O, $(NH_4)_2S_2O_8$, 72 °C; (b) morpholine, *i*-Pr_2NEt, dioxane, reflux; (c) HCO_2NH_4, Pd/C, MeOH, 48 °C; (d) butyl iodide, CH_3CN, reflux; (e) diethyl acetylenedicarboxylate, TBAF, THF, EtOH, reflux.

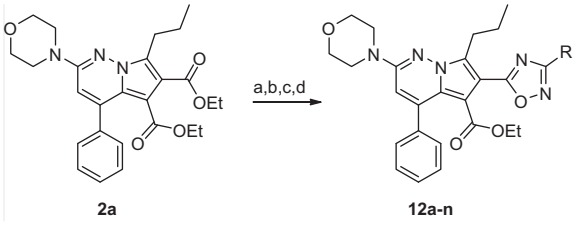

Scheme 3. Reagents and conditions: (a) NaOH, EtOH, H_2O, reflux; (b) $(COCl)_2$, DMF (cat), CH_2Cl_2; (c) $RC(=NOH)NH_2$, NEt_3, THF; (d) TBAF, THF.

alkyl groups such as cyclopropyl **2i** and cyclobutyl **2j** were less preferred in this position. The 7-ethyl derivative **2d** also retained activity but shortening the 7-alkyl group to methyl **2c** and deleting the group altogether **2b** caused a significant loss in DGAT1 inhibitory activity. Allyl analog **2e** was the most potent in the alkyl series, possibly due to its increased ability to form van der Waals interactions through its diffuse π-electron cloud.

Heteroatoms were tolerated in the alkyl chain as demonstrated by the DGAT1 IC_{50} values of ethers **2l** and **2m**; however, introduction of significant polarity as with an alkyl alcohol **2k** or alkyl amine **2n** completed abrogated DGAT1 inhibitory activity.

Replacement of the propyl group in **2a** by aryl groups was well tolerated and in fact the *para*-methoxyphenyl derivative **2t** is the most potent analog in the series. *para*-Substitution was preferred over *meta*-substitution in all cases tested as exemplified by *meta*-methoxyphenyl derivative **2p** being about 10-fold less potent than **2t**. The *para*-position of the phenyl ring tolerated a wide variety of substituents excluding polar groups as shown by the reduced inhibitory activity of the phenol **2s** and the aniline **2u**.

The bulk of the data indicates that the optimal groups at C7 are hydrophobic and capable of forming van der Waals interactions. Any significant polarity dramatically reduces DGAT1 inhibitory activity. Furthermore, this area of the binding pocket is able to accommodate very large groups as shown by analog **2w**, which possesses a *para*-benzyloxyphenyl group. There may however be a fairly narrow channel as analogs that force groups orthogonal to the phenyl ring such as **2v** or have any branching close to the pyrrolopyridazine core such as cycloalkyl derivatives **2i** and **2j** have significantly reduced DGAT1 IC_{50} values.

Changes at C2 of pyrrolopyridazine **2a** proved to be much less tolerated than at C7. This area of the molecule appeared to have very strict steric parameters in order to retain DGAT1 inhibitory activity. Simply replacing the morpholino ring of **2a** with a piperidinyl group such as in **9d** resulted in a 50-fold reduction in potency. Similarly, 2,6-dimethylmorpholine derivative **9a** proved to be at least 24-fold less potent than **2a**. In contrast, sterically less demanding groups such as pyrrolidine analog **9c** retained potency while azetidine **9b** and dimethylamine derivative **9e** were moderately potent.

All alkyl replacements of the phenyl group at C4 of **2a** provided analogs that were unable to inhibit DGAT1 activity at concentrations up to 3 μM (analogs **9i–m)**. Furthermore, replacement of any of the phenyl hydrogens of **2a** resulted in decreased DGAT1 inhibitory activity (analogs **9f–h**).

There are many heterocyclic bioisosteric replacements for esters reported in the literature.[20] We evaluated the ability of 5-methyloxazole, 5-methyl-1,3,4-oxadiazole and 3-methyl-1,2,4-oxadiazole to act as such replacements for the ethyl ester at C6 of pyrrolopyridazine **2a**. All three of these heterocycles possessed some DGAT1 inhibitory activity with 3-methyl-1,2,4-oxadiazole **12a** being the most potent inhibitor (data not shown). Further exploration of the SAR of the 1,2,4-oxadiazoles resulted in compounds **12b–n** (Table 3).

Propyl analog **12c** was the most potent inhibitor of the unbranched alkyl derivatives with the butyl derivative **12e** being essentially equipotent. Longer chains such as pentyl **12g** or shorter chains such as ethyl **12b** caused DGAT1 inhibitory activity to decrease slightly while the methyl derivative **12a** was about a sixfold weaker DGAT1 inhibitor. Branched and cyclic alkyl groups proved to be quite potent with the *t*-butyl **12f** and cyclopentyl **12j** analogs possessing DGAT1 IC_{50} values of 48 nM. Compounds possessing hydrophilic groups such as amines **12l** and **12m**, as well as hydroxyl groups **12n** showed decreased DGAT1 inhibitory activity. The oxadiazoles were evaluated in a DGAT1 cellular assay[16] to determine the amount of triglyceride uptake into CaCO2 cells. All of the oxadiazole analogs tested in the cell-based assay possessed similar IC_{50} values to that determined in the biochemical assay.

Table 3
DGAT1, CaCO2 and ACAT1 IC_{50} values of **12a–n**

Compd	R	DGAT1 IC_{50} (μM)	CaCO2 IC_{50} (μM)	ACAT1 IC_{50} (μM)
12a	Methyl	0.38		
12b	Ethyl	0.11		<1
12c	Propyl	0.065		0.26
12d	*i*-Propyl	0.057	0.051	<1
12e	Butyl	0.073	0.069	<1
12f	*t*-Butyl	0.048	0.019	0.083
12g	Pentyl	0.11		<1
12h	Phenyl	0.18	0.2	1.59
12i	Benzyl	0.12		0.077
12j	Cyclopentyl	0.048	<0.03	0.23
12k	Cyclohexyl	0.056	0.031	0.69
12l	Pyrrolidin-1-yl	0.10	0.10	0.77
12m	Dimethylamino	0.14		0.19
12n	2-OH-ethyl	0.18	0.26	1.05

Early selectivity studies indicated that pyrrolotriazine **1** and pyrrolopyridazine **2a** did not inhibit DGAT2; whereas, they potently inhibited ACAT1. Pyrrolopyridazine **2a** is about 11-fold selective for DGAT1 over ACAT1. Replacement of the 7-propyl group of **2a** with the methoxymethyl group in **2l** provided 36-fold DGAT1 selectivity compared to ACAT1 and was the most selective compound prepared. The *para*-methoxyphenyl analog **2t** and the allyl analog **2e** also had improved selectivities of 12- and 19-fold, respectively. Alterations of the morpholine at C2 failed to provide an increase in DGAT1 selectivity. Pyrrolidine **9c** had similar DGAT1 selectivity compared to **2a** while the dimethylamino derivative **9e** showed increased activity for ACAT1 over DGAT1. The oxadiazole analogs also had a range of DGAT1 selectivities including nine- and 12-fold selectivity for phenyl analog **12h** and cyclohexyl analog **12k**, respectively; whereas, benzyl analog **12i** possessed a lower IC_{50} for ACAT1 than for DGAT1.

In summary, novel DGAT1 inhibitor pyrrolotriazine **1** was discovered. Design of pyrrolopyridazine **2a** and systematic investigation of the SAR resulted in the finding that groups having π-electron density such as allyl, phenyl, and 4-substituted phenyls increased DGAT1 potency relative to the original propyl group at C7 of **2a**. The morpholino substituent at C2 and the phenyl ring at C4 of pyrrolopyridazine **2a** proved to be optimal within the series described in this report. It was discovered that the ethyl ester at C6 could be replaced by oxadiazoles **12** resulting in an increase in DGAT1 inhibitory activity. In fact, the *t*-butyl **12f** and cyclopentyl **12j** analogs are the most potent DGAT1 inhibitors described in this report with DGAT1 IC_{50} values of 48 nM. Selectivity for DGAT1 over ACAT1 was modestly increased for methoxymethyl analog **2l** and allyl analog **2e** but for the majority of compounds selectivity did not improve.[21]

References and notes

1. Chen, H. C.; Farese, R. V., Jr. *Trends Cardiovasc. Med.* **2000**, *10*, 188.
2. Farese, R. V., Jr.; Cases, S.; Smith, S. J. *Curr. Opin. Lipidol.* **2000**, *11*, 229.
3. Cases, S.; Smith, S. J.; Zheng, Y.-W.; Myers, H. M.; Lear, S. R.; Sande, E.; Novak, S.; Collins, C.; Welch, C. B.; Lusis, A. J.; Erickson, S. K.; Farese, R. V., Jr. *Proc. Natl. Acad. Sci. U.S.A.* **1998**, *95*, 13018.
4. Lardizabal, K. D.; Mai, J. T.; Wagner, N. W.; Wyrick, A.; Voelker, T.; Hawkins, D. J. *J. Biol. Chem.* **2001**, *276*, 38862.
5. Cases, S.; Stone, S. J.; Zhou, P.; Yen, E.; Tow, B.; Lardizabal, K. D.; Voelker, T.; Farese, R. V., Jr. *J. Biol. Chem.* **2001**, *276*, 38870.
6. Smith, S. J.; Cases, S.; Jensen, D. R.; Chen, H. C.; Sande, E.; Tow, B.; Sanan, D. A.; Raber, J.; Eckel, R. H.; Farese, R. V., Jr. *Nat. Genet.* **2000**, *25*, 87.
7. Chen, H. C.; Smith, S. J.; Ladha, Z.; Jensen, D. R.; Ferreira, L. D.; Pulawa, L. K.; McGuire, J. G.; Pitas, R. E.; Eckel, R. H.; Farese, R. V., Jr. *J. Clin. Invest.* **2002**, *109*, 1049.
8. Kahn, R. C. *Nat. Genet.* **2000**, *25*, 6.
9. Yanovski, S. C.; Yanovski, J. A. *N. Eng. J. Med.* **2002**, *346*, 591.
10. Lewis, G. F.; Carpentier, A.; Adeli, K.; Giacca, A. *Endocr. Rev.* **2002**, *23*, 201.
11. Brazil, M. *Nat. Rev. Drug Disc.* **2002**, *1*, 408.

12. Malloy, M. J.; Kane, J. P. *Adv. Inter. Med.* **2001**, *47*, 111.
13. Subauste, A.; Burant, C. F. *Curr. Drug Targets Immune Endocr. Metabol. Disord.* **2003**, *3*, 263.
14. Yu, Y.-H.; Ginsberg, H. *Ann. Med.* **2004**, *36*, 252.
15. DGAT1 was cloned from a human liver cDNA library. PCR was used to add a restriction site and flag epitope at the most 5′end and a restriction site at the 3′ end of the sequence. Thereafter, human flagtag (FT) DGAT1 baculovirus was generated using a Bac-to-Bac Baculovirus Expression System® (Invitrogen). Insect cells (e.g., sf9, sf2 1, or High Five) were infected for 24–72 h and collected by centrifugation. Cell pellets were re-suspended in homogenization buffer and lysed using a homogenization device, such as a microfluidizer. Total cell membranes were collected by ultracentrifugation at 45,000 rpm for 1 h. A small aliquot (0.2 μg/well) of membrane was incubated with varying concentrations of compound or mercuric chloride (as positive control for inhibition) in the presence of enzyme substrate, dioleoyl glycerol (200 μM) in 384-well plates, final volume 50 μL per well. The reaction was started by the addition of radioactive substrate, ^{14}C acyl coenzyme A (25 μM, such as decanoyl CoA, palmitoyl CoA, oleoyl CoA), and incubated at room temperature for 2 h. The reaction was stopped by adding Wheat Germ Agglutinin (WGA) SPA beads (0.2 mg) in mercuric chloride. Cell membranes were allowed to couple to the beads overnight. The signal was measured using a TopCount device.
16. Human colon tumor CaCO2 cells were cultured until confluent in 24-well plates. The medium was replaced with serum-free medium and the cells incubated for a further 24 h. Medium was replaced with serum-free medium containing 400 μM oleic acid (complexed with BSA, 2:1 mol/mol) and compound at varying doses in a final volume of 200 μl per well. Cells were incubated for 30 min before adding 0.1 μCi of ^{14}C oleic acid directly to the cells and the incubation continued for 30 min. Cells were washed two times with 1 ml PBS and air-dried at 37 °C for 10 min. Cell lipids were extracted with 0.5 ml hexane/isopropyl alcohol (3:2 v/v) for 5 min twice. Lipid extracts were evaporated to dryness, dissolved in chloroform and the lipid classes were resolved by TLC using hexane/ether/glacial acetic acid (80:20:1 v/v/v). The plates were exposed to a phosphorimager screen and the amount of radioactivity incorporated in to the triglyceride fraction was determined.
17. Full length human ACAT1 was cloned and modified by PCR to add a restriction site and flag epitope at the most 5′ end and a restriction site at the 3′ end of the sequence. Thereafter, human flagtag (FT) ACAT1 baculovirus was generated using a Bac-to-Bac Baculovirus Expression System® (Invitrogen). Insect cells, sf21, were infected for 24–72 h and collected by centrifugation. Cell pellets were re-suspended in homogenization buffer and lysed using a homogenization device, such as a microfluidizer. Total cell membranes were collected by ultracentrifugation at 45,000 rpm for 1 h. Membrane (0.5–2 μg) was incubated with varying concentrations of compound or SA-58035 (5–50 nM, as positive control for inhibition) in the presence of substrate, cholesterol/cyclodextrin (500 μM cholesterol), in microfuge tubes at a final volume of 100 μL. The reaction was started by the addition of radioactive substrate, ^{14}C palmitoyl CoA (25 μM), and incubated at ambient temperature for 10 min. The reaction was stopped by adding chloroform (1 mL) and vortexing. After brief centrifugation, the upper aqueous phase was removed and the organic phase applied to an aminopropyl Sep-Pak cartridge. Radioactive product, cholesterol palmitate, was eluted with chloroform (1 mL) into a scintillation vial and counted.
18. Kanemasa, S.; Kobira, S.; Kajigaeshi, S. *Heterocycles* **1980**, *14*, 1107.
19. Samaritoni, J. G. *Org. Prep. Proced. Int.* **1988**, *20*, 117.
20. Patani, G. A.; LaVoie, E. J. *Chem. Rev.* **1996**, *96*, 3147.
21. ACAT1 activity would presumably not pose a problem in a clinical setting, see example, Chang, C.; Dong, R.; Miyazaki, A.; Sakashita, N.; Zhang, Y.; Liu, J.; Guo, M.; Li, B.-L.; Chang, T.-Y. *Acta Biochim. Biophys. Sin.* **2006**, *38*, 151.